Dyes and Pigments 96 (2013) 16–24

Contents lists available at SciVerse ScienceDirect

Dyes and Pigments

journal homepage: www.elsevier.com/locate/dyepig

β-Carotene: A green, inexpensive, and convenient solvatochromic probe for the determination of solvent polarizability

Carina Loffredo, Paulo Augusto R. Pires, Muhammad Imran, Omar A. El Seoud*

Institute of Chemistry, University of São Paulo, P. O. Box 26077, 05513-970 São Paulo, SP, Brazil

ARTICLE INFO

Article history:
Received 30 May 2012
Received in revised form
18 July 2012
Accepted 19 July 2012
Available online 3 August 2012

Keywords:
Solvatochromism
β-Carotene solvatochromism
2-Alkoxyethanols polarizability
Ionic liquids polarizability
Solvatochromic probes
Solvation free energy relationships

ABSTRACT

Solvent polarizability has been previously determined by using the solvatochromic probe 3,20-di-*tert*-butyl-2,2,21,21-tetramethyl-3,5,7,9,11,13,15,17,19-docosanonaene whose synthesis involves 15 steps. We show here that the natural dye β-carotene, 1,1′-(3,7,12,16-tetramethyl-1,3,5,7,9,11,13,15,17-octadecanonaene-1,18-diyl)bis[2,6,6-trimethylcyclohexene], can be conveniently employed for the accurate determination of the same solvent property. This conclusion is based on both theoretical calculations and experimental data. The former includes free energies of solvation, and the wavenumber of the longest wavelength (i.e., the solvatochromic) transition. Both quantities for β-carotene correlate linearly with the corresponding values of the docosanonaene, with slopes and correlation coefficients of practically unity. The plot of experimentally calculated solvent polarizability of β-carotene versus that of the docosanonaene was found to be linear for 68 solvents. Previously unknown solvent polarizability values are reported for eight $ROCH_2CH_2OH$ ($R = C_1$ to C_{10}) and four 1-allyl-3-R-imidazolium chloride ionic liquids ($R = C_6$ to C_{10}). The dependence of solvent polarizability on the number of carbon atoms in the hydrocarbon chains of several classes of solvents is calculated, it shows the importance of van der Waals interactions in ionic liquids.

1. Introduction

The influence of solvents on chemical phenomena (rate and equilibrium constants; spectroscopic transitions, etc.) are usually analyzed in terms of linear combinations of solvent parameters, e.g.:

$$\text{Effect of solvent} = a\,\mathrm{SA} + b\,\mathrm{SB} + d/p\,\mathrm{S(D/P)} \qquad (1)$$

where (S) refers to solvent; (A, B, D/P) refer to solvent "acidity", "basicity", and "dipolarity/polarizability", and (a, b, d/p) are the corresponding regression coefficients. These represent the susceptibility of the phenomenon in question to the particular solvent property [1,2].

The values of the solvent descriptors in Eqn. (1) are most readily calculated by manipulating the Uv–vis spectra, absorption or emission, of solvatochromic substances (hereafter designated as "probes"). The spectra of these compounds are responsive to the properties of the medium. Because these probes are sensitive, *to varying extents*, to more than one solvent property, the information required is obtained by manipulating the spectra of pairs of homomorphs (molecules that have the same, or a closely related molecular structures, e.g., 4-nitroaniline and *N*,*N*-dimethyl-4-nitroaniline for the calculation of SB). Fig. 1 shows typical examples of such solvatochromic probes. Of these, RB is employed for the determination of the *overall* empirical solvent polarity scale $E_T(30)$, that is the sum of the three left-hand parameters of Eqn. (1).

In Eqn. (1) the "cavity" term has been omitted, because the excitation of these probes obeys the Frank–Condon principle. Another variety of Eqn. (1) includes the term log P, for solvent lipophilicity (=partition coefficient of the solvent between water and 1-octanol, both mutually saturated) [3]. This descriptor is required in order to describe the solvatochromism of certain probes, e.g., merocyanines [4].

Catalán and Hopf, have shown that it is possible to separate solvent dipolarity from its polarizability, by using the probe ttbP9. In this case, the last term of Eqn. (1) should be expanded to (d SD + p SP) [5,6]. This is an interesting approach in view of the importance of van der Waals interactions for diverse phenomena, *inter alia*, the properties and solubilization of biopolymers in ionic liquids, ILs [7–9], and the precipitation of petroleum asphaltenes [10]. Obtaining ttbP9 is, however, a major synthetic undertaking, involving an expensive, laborious route, composed of fifteen steps [11]. For example, the cost of chemicals for obtaining 1 g of certain

---

* Corresponding author. Tel./fax: +55 11 3091 3874.
E-mail address: elseoud@iq.usp.br (O.A. El Seoud).

0143-7208/$ – see front matter © 2012 Elsevier Ltd. All rights reserved.
http://dx.doi.org/10.1016/j.dyepig.2012.07.017

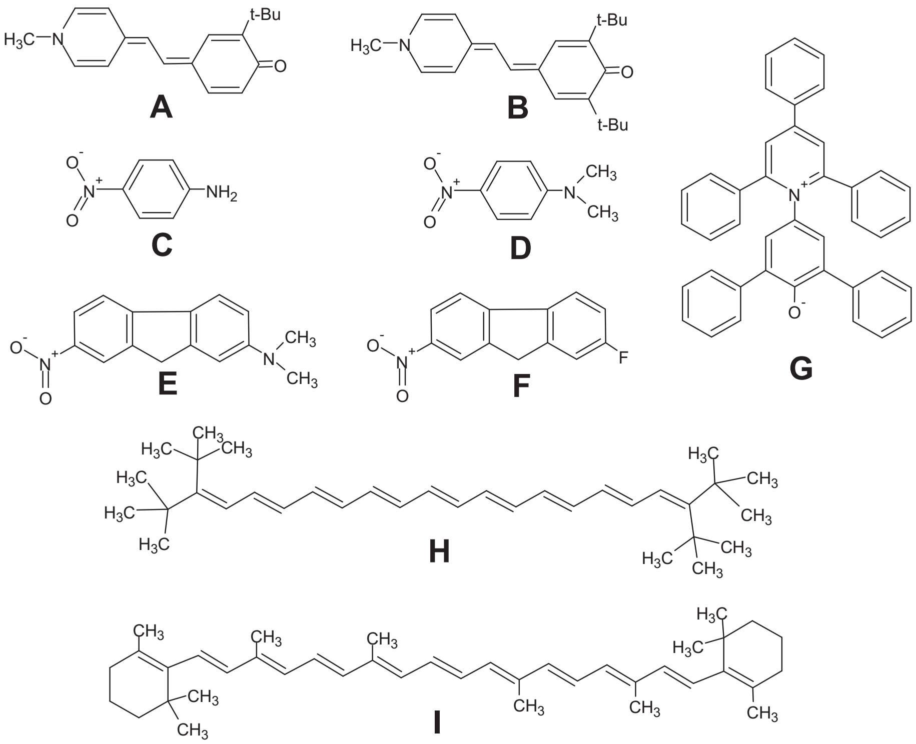

Fig. 1. Typical examples of the probes that are employed for the determination of the solvent descriptors of Eqn. (1). These include the pairs of homomorphs: *o-tert*-butylstilbazolium betaine (A) and *o,o′*-di-*tert*-butylstilbazolium betaine (B) (SA); 4-nitroaniline (C) and *N,N*-dimethyl-4-nitroaniline (D) (SB); 2-(*N,N*-dimethylamino)-7-nitrofluorene (E) and 2-fluoro-7-nitrofluorene (F) (D/P). The probes 2,6-diphenyl-4-(2,4,6-triphenylpyridinium-1-yl) phenolate (RB) (G); 3,20-di-*tert*-butyl-2,2,21,21-tetramethyl-3,5,7,9,11,13,15,17,19-docosanonaene, ttbP9 (H); and (all *trans*) 1,1′-(3,7,12,16-tetramethyl-1,3,5,7,9,11,13,15,17-octadecanonaene-1,18-diyl)bis[2,6,6-trimethylcyclohexene], β-carotene (I) are employed for the determination of the empirical solvent (overall) polarity, and polarizability, *vide infra*.

intermediates (compound **27b** from compound **23**) is ca. 65 times the cost of 1 g of a good commercial grade of β-carotene [11]. These difficulties are manifested by the fact that the only experimental data about (SP) came from Catalán's and Hopf's research groups [5,6,11,12].

Fig. 1 shows that ttbP9 and β-carotene have similar polyene systems and should, in principle, be sensitive to solvent polarizability to the same extent. Indeed, solvent effects on the Uv–vis spectrum of β-carotene have been the subject of several theoretical studies [13–17], and experimental ones for both pure solvents [18,19], and binary mixtures [20,21]. The result of these studies – that are relevant to the present one – is that the wavenumber of the visible absorption maximum of the longest wavelength transition, correlate linearly with the solvent Lorenz–Lorentz refractive index (n) function, $f(n^2) = (n^2 - 1)/(n^2 + 2)$; deviations occur in the media containing high proportion of F, Cl or S atoms, having very different polarizability densities, as compared to (common) H, C, N and O.

With this background, and taking into account that natural β-carotene is a green probe, readily available at low cost, we decided to determine its use as a convenient substitute for ttbP9. We have expanded the list of solvents for which the values of $SP_{\beta\text{-carotene}}$ are available by additional 38 solvents, including the industrially important 2-alkoxyethanols, $ROCH_2CH_2OH$ (where R = C_1 to C_{10}); and the ionic liquids, ILs (whose polarizability has been determined for the first time) 1-R-3-allylimizalolium chloride (where R = C_6 to C_{10}).

Our results for several molecular solvents were found to be in excellent agreement with those reported by Abboud et al.; the values of $\tilde{\nu}_{\text{max, }\beta\text{–carotene}}$ and $\tilde{\nu}_{\text{max, ttbP9}}$ for 68 solvents, hence the corresponding SP values, were found to correlate linearly with slope and correlation coefficient, r, of practically unity. That is, both probes can be conveniently employed in order to determine (SP). This conclusion is corroborated by the results of theoretical calculations that showed perfect linear correlation between values of $\tilde{\nu}_{\text{max, }\beta\text{–carotene, calculated}}$ and $\tilde{\nu}_{\text{max, ttbP9, calculated}}$ for 23 solvents. Finally, for solvent homologous series (1-alkanes, $ROCH_2CH_2OH$; ROH; ILs) the dependence of (SP) on the number of carbon atoms (N_C) in the longest carbon-chain has been calculated and analyzed.

2. Materials and methods

2.1. Chemicals

The chemicals were purchased from Alfa-Aeser, Merck, or Δ-PAC2 Química; the solvents were purified as given elsewhere [22] and stored over activated type 4 Å molecular sieves; RB was that available from a previous study [23]. The purity of the solvents was established by comparing their densities (DMA4500 digital density meter, Anton Paar, Graz), and $E_T(30)$ with literature values [2,24].

The probe β-carotene (Fluka, purity ≥ 97.0%) was employed either as received, or after purification by crystallization from ethanol/toluene. Both samples were divided into small portions, put into tightly-stoppered glass vials, and stored at ca. −18 °C until used. *All* manipulation of this probe has been carried out under nitrogen, in absence of direct light.

2.2. Synthesis

2.2.1. 2-Alkoxyethanols [25]

The following is a general procedure: to a 3-necked round-bottom flask, provided with a reflux condenser, dropping funnel, and inlet for dry nitrogen was added 50 g (0.8 mol) of dry ethylene glycol. Small pieces of sodium (0.29 mol, 6.8 g), were slowly added to the glycol under vigorous magnetic stirring and the mixture was heated to 60 °C until the sodium dissolved. The appropriate 1-bromoalkane

(0.25 mol for each RBr, 37.76 g; 41.27 g; 48.28 g; 55.30 g for R = C_5; C_6; C_8 and C_{10}, respectively) was added slowly (*ca.* 30 min) and the solution was then kept under reflux for the appropriate time (1 h; 3 h; and 4 h for R = C_5; C_6; C_8 and C_{10}, respectively). The precipitated NaBr was filtered off and the residue was washed with water; the upper layer was separated and dried with anhydrous $MgSO_4$, and the product purified by fractional distillation.

The boiling points and densities of the solvents were in good agreement with literature values [25]. The ^1H NMR data (Bruker DPX-300 NMR spectrometer, 300 MHz for ^1H; $CDCl_3$; δ in ppm, J in Hz) of the synthesized 2-alkoxyethanols are listed below, the numbering of atoms is shown in Fig. 2.

2.2.1.1. 2-Pentyloxyethanol

Colorless liquid: $C_5H_{11}OCH_2CH_2OH$; yield: 16 g (46%); b.p.: 186–187 °C/753 torr; d_4^{20}: 0.8917; ^1H NMR: 0.91 (3H, t, J = 8.0, H7), 1.29–1.37 (4H, m, H6), 1.61 (2H, t, J = 6.0, H5), 3.51 (4H, m, H2, 4), 3.72 (2H, t, J = 6.0, H3), 2.91 (1H, H1).

2.2.1.2. 2-Hexyloxyethanol

Colorless liquid: $C_6H_{13}OCH_2CH_2OH$; yield: 22 g (59%); b.p.: 111–113 °C/27 torr; d_4^{20}: 0.8859; ^1H NMR: 0.91 (3H, t, J = 8.0, H7), 1.29–1.36 (6H, bs, H6), 1.60 (2H, t, J = 6.0, H5), 3.52 (4H, m, H2, 4), 3.73 (2H, t, J = 6.0, H3), 2.86 (1H, H1).

2.2.1.3. 2-Octyloxyethanol

Colorless liquid: $C_8H_{17}OCH_2CH_2OH$; yield: 24 g (55%); b.p.: 130–132 °C/22 torr; d_4^{20}: 0.8795; ^1H NMR: 0.91 (3H, t, J = 8.0, H7), 1.29–1.36 (6H, bs, H6), 1.60 (2H, t, J = 6.0, H5), 3.52 (4H, m, H2, 4), 3.73 (2H, t, J = 6.0, H3), 2.86 (1H, H1).

2.2.1.4. 2-Decyloxyethanol

Colorless liquid: $C_{10}H_{21}OCH_2CH_2OH$; yield: 23 g (45%); b.p.: 156–157 °C/20 torr; d_4^{20}: 0.8715; ^1H NMR: 0.92 (3H, t, J = 8.0, H7), 1.23–1.36 (14H, bs, H6), 1.79 (2H, t, J = 6.0, H5), 3.45 (4H, m, H2, 4), 3.58 (2H, t, J = 6.0, H3), 2.17 (1H, H1).

2.2.2. N-(1-alkyl)imidazoles

These compounds were obtained from the reaction of the sodium salt of imidazole and 1-bromoalkanes, as follows: to a 3-necked round-bottom flask, provided with a reflux condenser, dropping funnel, and inlet for dry nitrogen was added a solution of imidazole (7.49 g; 0.11 mol) in dry ethanol (25 mL). Small pieces of sodium (2.53 g, 0.11 mol), were slowly introduced, the mixture was vigorously stirred until the metal has dissolved and then heated under reflux for 2 h. The mixture was cooled to room temperature; the appropriate 1-bromoalkane (0.10 mol; 16.50 g, 17.91 g, 19.31 g, 22.12 g for R = C_6; C_7; C_8 and C_{10}, respectively) was added slowly (*ca.* 30 min); then the mixture was refluxed for 2 h. The mixture was cooled to room temperature, the precipitated NaBr was filtered off; the ethanol evaporated, the residual oil was washed with water, and then dried with anhydrous $MgSO_4$. The *N*-(1-alkyl)imidazoles were purified by fractional distillation (yields before distillation *ca.* 98%); their purity was confirmed with ^1H NMR spectroscopy (results not shown).

2.2.3. 1-Allyl-3-R-imidazolium chlorides for R = C_6; C_7; C_8 and C_{10}

These ILs were obtained by the reaction of the appropriate *N*-(1-alkyl)imidazole with allyl chloride (3-chloro-1-propene), under microwave (MW) irradiation as follows, for 1-allyl-3-(1-hexyl)imidazolium chloride, AlHxImCl; 1-allyl-3-(1-heptyl)imidazolium chloride, AlHpImCl; 1-allyl-3-(1-octyl)imidazolium chloride AlOcImCl; 1-allyl-3-(1-decyl)imidazolium chloride, AlDcImCl. *N*-(1-alkyl)imidazole (0.22 mol; 33.49 g, 36.58 g, 39.66 g, 45.8 g for R = C_6; C_7; C_8 and C_{10}) and 3-chloro-1-propene (0.25 mol; 19.13 g) were mixed in a glass reactor, provided with a reflux condenser and inlet for dry nitrogen; the reactor was introduced in the cavity of the MW apparatus (Discover model DU-8316; CEM; Matthews) and irradiated under vigorous stirring for 1 h; 20 W, 80 °C.

The product was dissolved in ethyl acetate (100 mL); the solution placed in a freezer (phase separation of the IL); the upper layer discarded; this process was repeated thrice. After removal of ethyl acetate, the IL was dried at 110 °C, 1 mmHg for 12 h. The yields were 98 ± 1% (light yellow viscous liquid in all cases).

For elemental analyses, the (hygroscopic) ILs were transformed into their (non-hygroscopic) perchlorate counterparts, as follows: to a solution containing 0.5 g of the IL in 5 mL water was added 5 mL of an aqueous solution containing 0.5 g $NaClO_4$. The IL perchlorate (colorless viscous liquids) were suspended in water several times; the water was separated; and the IL dried at 40 °C, under reduced pressure, over P_4O_{10} until constant weight. The results of elemental analyses and the ^1H NMR data of AlRImCl (Bruker DRX-500 NMR spectrometer; 500 MHz for ^1H; $CDCl_3$; δ in ppm, J in Hz) are listed below; Fig. 3 shows the numbering of the hydrogen atoms.

2.2.3.1. 1-Allyl-3-(1-hexyl)imidazolium chloride

Light-yellow, viscous liquid. ^1H NMR for $C_{12}H_{21}N_2Cl$: 0.88 (3H, t, J = 7.0, H_{13}), 1.27–1.40 (6H, m, H_{12}), 1.78–1.97 (2H, m, H_{11}), 4.34 (2H, t, J = 7.7, H_{10}), 5.07 (2H, d, J = 6.6, H_6), 5.46 (1H, d, J = 4.2, H_9), 5.49 (1H, s, H_8), 6.03 (1H, m, H_7) 7.25 (2H, s, H_4 & H_5), 10.98 (1H, s, H_2). Calcd. for $C_{12}H_{21}N_2ClO_4$: C, 49.2%; H, 7.2%; N, 9.6%. Found: C, 49.1%; H, 7.2%; N, 9.7%.

2.2.3.2. 1-Allyl-3-(1-heptyl)imidazolium chloride

Light-yellow, viscous liquid. ^1H NMR for $C_{13}H_{23}N_2Cl$: 0.88 (3H, t, J = 7.0, H_{13}), 1.27–1.40 (8H, m, H_{12}), 1.82–1.97 (2H, m, H_{11}), 4.34 (2H, t, J = 7.7, H_{10}), 5.07 (2H, d, J = 6.6, H_6), 5.46 (1H, d, J = 4.2, H_9), 5.49 (1H, s, H_8), 6.03 (1H, m, H_7) 7.25 (2H, s, H_4 & H_5), 10.96 (1H, s, H_2). Calcd. for $C_{13}H_{23}N_2ClO_4$: C, 50.9%; H, 7.6%; N, 9.1%. Found: C, 50.9%; H, 7.6%; N, 9.2%.

2.2.3.3. 1-Allyl-3-(1-octyl)imidazolium chloride

Light-yellow, viscous liquid. ^1H NMR for $C_{14}H_{25}N_2Cl$: 0.88 (3H, t, J = 7.0, H_{13}), 1.20–1.39 (10H, m, H_{12}), 1.88–1.96 (2H, m, H_{11}), 4.34 (2H, t, J = 7.4, H_{10}), 5.07 (2H, d, J = 6.5, H_6), 5.46 (1H, m, H_9), 5.48 (1H, m, H_8), 6.03 (1H, m, H_7) 7.26 (2H, s, H_4 & H_5), 10.93 (1H, s, H_2). Calcd. for $C_{14}H_{25}N_2ClO_4$: C, 52.4%; H, 7.9%; N, 8.7%. Found: C, 52.5%; H, 7.9%; N, 8.8%.

2.2.3.4. 1-Allyl-3-(1-decyl)imidazolium chloride

Light-yellow, viscous liquid. ^1H NMR for $C_{16}H_{29}N_2Cl$: 0.88 (3H, t, J = 7.2, H_{13}), 1.19–1.40 (14H, m, H_{12}), 1.92 (2H, *dxt*, J = 7.4, H_{11}), 4.33 (2H, t, J = 7.6, H_{10}), 5.07 (2H, d, J = 6.5, H_6), 5.46 (1H, d, J = 7.6, H_9), 5.48 (1H, s, H_8), 6.02 (1H, m, H_7) 7.20 (2H, s, H_4 & H_5), 11.03 (1H, s, H_2). Calcd. for $C_{16}H_{29}N_2ClO_4$: C, 55.1%; H, 8.4%; N, 8.0%. Found: C, 55.1%; H, 8.5%; N, 8.1%.

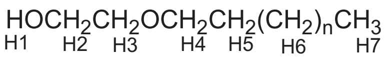
$HOCH_2CH_2OCH_2CH_2(CH_2)_nCH_3$

Fig. 2. Numbering of the hydrogen atoms of 2-alkoxyethanols.

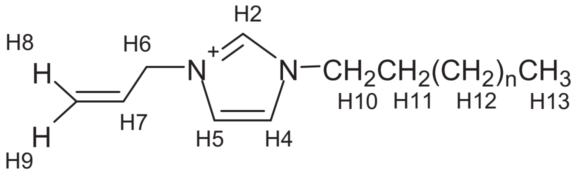

Fig. 3. Numbering of the hydrogen atoms of the ionic liquid cation.

2.3. Uv–visible spectroscopic measurements

These have been carried out at 25 ± 0.1 °C by using a Shimadzu UV-2500 spectrophotometer, equipped with a model 4029 digital thermometer (Control Company, Friendsmood), under the following experimental conditions: each spectrum was recorded at least thrice, at 140 nm/min; slit width 0.5 nm; sampling interval 0.2 nm. The accuracy of λ_{max} was routinely checked against the known peaks of a holmium oxide glass filter (model 666-F1, Hellma Analytics, Müllheim). Values of λ_{max} were determined from the first derivative of the absorption spectra, calculated by using the commercial software Grams/32 [26]; the uncertainty in λ_{max} is ±0.2 nm.

3. Results and discussion

Note: the procedures and equations that have been employed for all calculations are given in the "Calculations" section.

3.1. Relevance of the purity of β-carotene; agreement with previously published data

The deceptively simple task of obtaining highly pure β-carotene has been discussed in details elsewhere [27]. We have employed this probe with and without recrystallization. Impurities, if they are present or develop during probe manipulation, are not expected to affect our results, provided that they do not absorb at the same λ_{max} of the solvatochromic peak. The reason is that it is peak *position* (i.e., λ_{max}) and not *intensity* that is employed in calculating $\tilde{\nu}_{max}$, hence SP. The following has been done in order to assess whether it is appropriate to use β-carotene *as received*: the values of $\tilde{\nu}_{max,\ \beta-carotene}$, calculated from the spectra of recrystallized and non-crystallized samples were correlated, as shown by Eqn. (2), where r = correlation coefficient; sd = standard deviation; N_S = number of solvents employed:

$$\tilde{\nu}_{max,\ \beta-carotene}(\text{probe used as received}) = -754 + 1.03\ \tilde{\nu}_{max,\ \beta-carotene}(\text{recrystallized sample}), \quad r = 0.9984;\ \text{sd} = 18.4888;\ N_s = 8 \tag{2}$$

Additionally, we have plotted $\tilde{\nu}_{max,\ \beta-carotene}$ (sample used as received) against those published by Abboud et al., [19] (β-carotene recrystallized from benzene–methanol). As shown by Eqn. (3), both sets are in excellent agreement. In subsequent work, therefore, β-carotene has been employed as received.

$$\tilde{\nu}_{max,\ \beta-carotene}(\text{probe used as received}) = 237.27 + 0.9882\,\tilde{\nu}_{max,\ \beta-carotene}(\text{Abboud's data; recrystallized sample}); \quad r = 0.9985;\ \text{sd} = 15.617;\ N_s = 23 \tag{3}$$

3.2. Can β-carotene be reliably employed for the determination of solvent polarizability?

In order to answer this question, we have employed two strategies: (i) we compared theoretically calculated energies of solvation and ($\tilde{\nu}_{max}$), hence SP, of β-carotene and of ttbP9 for a large set of representative solvents; (ii) we have compared the corresponding experimental $\tilde{\nu}_{max}$ values.

3.2.1. Theoretical calculations

With regard to (i), the following procedure has been employed *for each probe*: its geometry in gas phase has been optimized; the geometry-optimized probe was solvated in 23 solvents, for which parameterized data are available in the software package employed (Gamess US, vide Calculations). The solvent set employed covers nonpolar and weakly polar aliphatic and aromatic hydrocarbons, dipolar aprotic solvents, and aliphatic alcohols. Gibbs free energies of solvation, and the values of $\tilde{\nu}_{max,\ \beta-carotene,\ Theo}$ and $\tilde{\nu}_{max,\ ttbP9,\ Theo}$ were compared. The results of these calculations are listed in Table 1.

At the outset, the quality of geometry optimization of both probes can be shown by the agreement between our calculated bond lengths and angles with those calculated by other authors, and with X-ray data, see Tables SM-1 and SM-2. Several points can be deduced from Table 1: (1) the values of $\Delta G_{solvation}$ for both solvents correlate linearly; (2) in any solvent, the solvation of β-carotene is more favorable than that of ttbP9; (3) the values of theoretically calculated and experimental values of $\tilde{\nu}_{max}$ are in reasonable agreement.

The first point is clear from Eqn. (4); it indicates that the energies of solvation of the two probes are similar.

$$\Delta G_{solvation,\ \beta-carotene} = -1.3464 + 1.1431\ \Delta G_{solvation,\ ttbP9} \quad (r = 0.9988;\ \text{sd} = 0.1899;\ N_s = 23) \tag{4}$$

The second point reflects the more lipophilic character of β-carotene, as shown by the corresponding values of log *P* [28]; 13.1 and 14.8 for ttbP9 and β-carotene, respectively. Because each probe carries a polyene chain consisting of 9 conjugated all-trans double bonds, then the difference must be due to the methyl groups on the polyene chain, plus the cyclohexene rings of β-carotene. This conclusion is corroborated by calculating Gibbs free energies of solvation (gas phase → solvent) of the compounds shown in Fig. 4; these model the termini of both probes.

The calculations showed that the solvation of compound **1** (model for the termini of β-carotene) is more favorable than that of **2** (model for the end groups of ttbP9). The corresponding values of $\Delta G_{solvation}$,

Table 1
Theoretically calculated Gibbs free energy of solvation, $\Delta G_{solvation}$, and values of $\tilde{\nu}_{max}$, for β-carotene and di-*tert*-butyl-tetramethyl-docosanonaene, ttbP9.

Solvent	β-carotene			ttbP9		
	$\Delta G_{solvation}$, kcal mol^{-1}	$\tilde{\nu}_{max}$, cm^{-1}	%$\Delta\tilde{\nu}_{max}$[a]	$\Delta G_{solvation}$, kcal mol^{-1}	$\tilde{\nu}_{max}$, cm^{-1}	%$\Delta\tilde{\nu}_{max}$[a]
Gas phase	–	22,443	−0.17	–	24,767	−3.30
n-Heptane	−22.31	21,215	4.25	−18.09	21,924	−0.88
Cyclohexane	−24.20	21,126	3.82	−20.01	21,841	−1.29
Dichloromethane	−25.93	21,113	2.41	−21.57	21,833	−2.56
Trichloromethane	−25.49	21,081	2.24	−21.05	21,791	−2.74
Tetra-chloromethane	−25.21	21,072	2.46	−20.60	21,777	−2.41
1,2-Dichloro ethane	−23.03	21,073	2.30	−19.00	21,785	−2.50
Benzene	−24.11	21,001	2.53	−19.56	21,696	−2.46
Nitromethane	−18.46	21,189	–	−15.13	21,915	−2.08
Acetonitrile	−20.79	21,269	3.67	−17.22	22,003	−1.40
Butanenitrile	−22.14	21,223	–	−18.37	21,954	−5.11
Pentanenitrile	−22.54	21,185	–	−18.70	21,914	−5.64
1,4-Dioxane	−13.24	21,142	2.67	−10.08	21,850	−1.62
THF	−20.49	21,152	3.00	−16.77	21,871	−1.94
Acetone	−21.86	21,239	3.49	−18.10	21,971	−5.30
DMSO	−12.64	21,118	1.04	−9.93	21,839	−3.77
DMF	−17.41	21,092	2.37	−14.10	21,809	−5.83
Methanol	−17.65	21,304	4.18	−14.40	22,038	−0.96
Ethanol	−18.77	21,234	3.97	−15.34	21,962	−1.39
1-Propanol	−18.53	21,184	3.82	−15.09	21,909	−1.19
1-Butanol	−18.01	21,156	3.71	−14.61	21,879	−1.31
1-Hexanol	−17.68	21,122	2.70	−14.27	21,841	−1.53
1-Octanol	−17.07	21,102	3.35	−13.71	21,818	−1.68
1-Decanol	−16.22	21,090	–	−12.92	21,805	−1.77

[a] $\%\Delta\tilde{\nu}_{max} = 100 \times (\tilde{\nu}_{max\ experimental} - \tilde{\nu}_{max\ Theo})/(\tilde{\nu}_{max\ experimental})$. The experimental data for β-carotene are listed in Table 2 below; those for ttbP9 are published elsewhere [5].

kcal/mol, are (β-carotene; ttbP9; solvent): −5.80, −4.51 (in benzene); −4.03, −2.85 (in 1-octanol); −3.12, −2.04 (in 1,4-dioxane).

For each probe, plot of theoretical versus experimental $\tilde{\nu}_{\text{max}}$ showed correlation coefficients of, after excluding the worst offenders (22% of the data), 0.8389 and 0.8217, for β-carotene and ttbP9, respectively.

A clear indication, however, that both probes are proportionally sensitive to solvent polarizability can be concluded from Fig. 5 that depicts the correlation of $\tilde{\nu}_{\text{max, }\beta\text{-carotene, Theo}}$ and $\tilde{\nu}_{\text{max, ttbP9, Theo}}$ for 23 solvents; the corresponding equation is:

$$\tilde{\nu}_{\text{max, }\beta-\text{carotene, Theo}} = 1574 + 0.895\,\tilde{\nu}_{\text{max, ttbP9, Theo}} \quad (r = 0.9974;\ \text{sd} = 5.2490;\ N_s = 23) \tag{5}$$

3.2.2. *Experimental data*

3.2.2.1. *Is the value of $\tilde{\nu}_{max}$ affected by the experimental conditions?*

The accuracy of the value of $\tilde{\nu}_{\text{max}}$ may be slightly affected if the peak full width at half height (FWHH), or its shape are noticeably dependent on experimental conditions, in particular the dye concentration, and the nature of the solvent [17]. Based on curve deconvolution (see item 5.3 in Calculations), we have found that *this is not the case*. For example, the FWHH is the same (uncertainty within 3%) for five different concentrations of β-carotene in isooctane [(1.6–16.1) × 10^{-5} mol/L]. For the same dyes concentration (1.2 × 10^{-5} mol/L) in 4 distinct solvents (hexane; dichloromethane, 1-hexanol, and THF) both peak shape and FWHH are the same (uncertainty in FWHH 1–4%). An example of these deconvolutions is shown in Fig. 6. Therefore, the experimental conditions have no bearing on the accuracy of $\tilde{\nu}_{\text{max}}$, hence on the calculated values of SP.

3.2.2.2. *Comparison of the experimental $\tilde{\nu}_{max, Exp}$, and the calculated SP values*

The experimental values of $\tilde{\nu}_{\text{max, }\beta-\text{carotene, Exp}}$, $\tilde{\nu}_{\text{max, ttbP9, Exp}}$ are listed in Table 2, along with the corresponding SP, and the refractive index (n).

Regarding these data, the following is relevant:

(i) The agreement between the results of the two probes can be demonstrated from plots of $\tilde{\nu}_{\text{max}}$ or SP, the latter is shown in Fig. 7; the corresponding correlations are given by:

$$\tilde{\nu}_{\text{max, }\beta-\text{carotene, Exp}} = -1348 + 1.08\,\tilde{\nu}_{\text{max, ttbP9, Exp}} \quad r = 0.9934;\ \text{sd} = 38.85;\ N_s = 68 \tag{6}$$

$$\text{SP}_{\beta-\text{carotene}} = -0.04 + 1.04\,\text{SP}_{\text{ttbP9}}, \quad r = 0.9934;\ \text{sd} = 0.0105;\ N_s = 68 \tag{7}$$

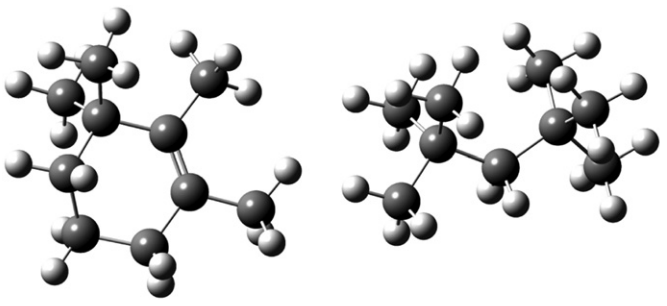

Fig. 4. Model compounds (1,2,3,3-tetramethylcyclohexene and 2,2,4,4-tetramethylpentane) employed for the calculation of Gibbs free energy of solvation of the termini of β-carotene and ttbP9, respectively.

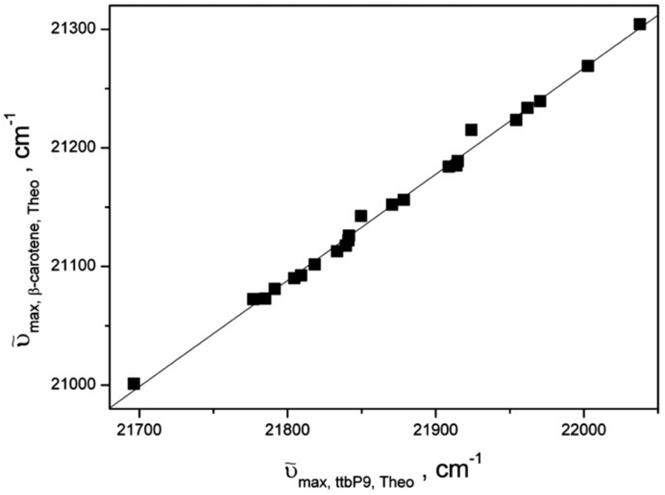

Fig. 5. Correlation between theoretically calculated transition energies, $\tilde{\nu}_{\text{max}}$, of ttbP9 and β-carotene.

Both results show that our initial expectation is confirmed, i.e., because the polyene systems are the same, both indicators respond similarly to solvent polarizability. Therefore *β-carotene is a convenient probe for SP as argued in Introduction*;

(ii) The above conclusion can be corroborated by comparing the dependences of SP and Lorenz–Lorentz refractive index function, *vide supra*, on the number of carbon atoms, N_C, of the aliphatic chain for series of homologous compounds, e.g., alkanes, see Eqns. (8) and (9):

$$\text{SP}_{\text{Alkanes, }\beta-\text{carotene}} = 0.46877 + 0.0263\,N_C - 0.0008\,N_C^2 \quad (r = 0.99154;\ \text{sd} = 0.00418;\ N_S = 8) \tag{8}$$

$$\text{Reduced}\,f(n^2)_{\text{Alkanes}} = 0.49956 + 0.0296\,N_C - 0.00094\,N_C^2 \quad (r = 0.99494;\ \text{sd} = 0.00345;\ N_S = 8) \tag{9}$$

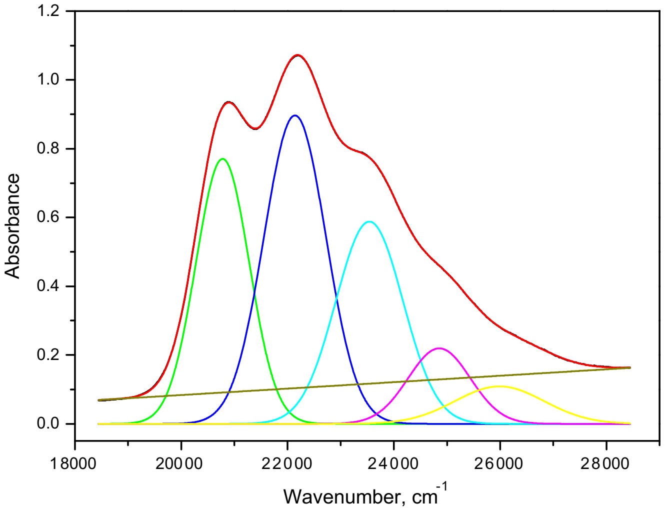

Fig. 6. Example of the deconvolution of the band of the longest wavelength transition of β-carotene. [β-carotene] = 1.2 × 10^{-5} mol L^{-1}, in isooctane. The upper curve represents an overlap between the calculated spectrum (red color; sum of the deconvoluted bands) and the experimental (black color, not seen because of overlap of the two curves). (For interpretation of the references to color in this figure legend, the reader is referred to the web version of this article.)

Table 2
Wavenumbers of the visible absorption maximum of the longest-wavelength transition, $\tilde{\nu}_{\mathrm{max}}$ of ttbP9 and β-carotene, the corresponding solvent polarizability (SPs) and the refractive index (n).

Entry	Solvent	$\tilde{\nu}_{\mathrm{max,\ ttbP9}}$, cm^{-1}[a]	$\tilde{\nu}_{\mathrm{max,\ \beta-carotene}}$, cm^{-1}	$\mathrm{SP}_{\mathrm{ttbP9}}$	$\mathrm{SP}_{\beta\text{-carotene}}$	n[a]
	Gas phase	23,975	24,402[c]	–	–	1
Aliphatic and alicyclic hydrocarbon						
1	*n*-Pentane	21,880	22,271[c]	0.5935	0.5803	1.358
2	3-Methylpentane	21,786[b]	22,251[d]	0.6201	0.5858	1.376
3	2,2,4-Trimethylpentane	21,793[b]	22,181[c]	0.6181	0.6048	1.392
4	*n*-Hexane	21,799	22,202[c]	0.6164	0.5991	1.375
5	Cyclohexane	21,564	21,964[c]	0.6830	0.6639	1.426
6	Methylcyclohexane	21,591	22,030[d]	0.6754	0.6460	1.399
7	*n*-Heptane	21,732	22,157[c]	0.6354	0.6114	1.387
8	*n*-Nonane	21,646	22,070[d]	0.6598	0.6351	1.405
9	*n*-Decane	21,614	21,985[c]	0.6688	0.6582	1.411
10	*n*-Dodecane	21,564	21,953[c]	0.6830	0.6669	1.422
11	*n*-Tetradecane	21,520	21,917[c]	0.6955	0.6767	1.429
12	*n*-Hexadecane	21,491	21,894[c]	0.7037	0.6830	1.434
13	Decalins (mixture)	21,350	21,788[d]	0.7436	0.7119	1.475
Halogenated compounds						
14	Dichloromethane	21,288	21,634[c]	0.7612	0.7538	1.424
15	Trichloromethane	21,210	21,564[c]	0.7833	0.7729	1.444
16	Tetrachloromethane	21,265	21,603[c]	0.7677	0.7623	1.460
17	1,2-Dichloroethane	21,253	21,570[c]	0.7711	0.7712	1.445
18	1-Chlorobutane	21,529	21,891[c]	0.6929	0.6838	1.402
19	Chlorobenzene	21,035	21,394[c]	0.8329	0.8192	1.524
20	Fluorobenzene	21,289	21,697[d]	0.7609	0.7367	1.465
21	Hexafluorobenzene	21,776	22,165[d]	0.6229	0.6092	1.377
Aromatic compounds						
22	Benzene	21,176	21,546[c]	0.7929	0.7778	1.501
23	Toluene	21,216	21,583[c]	0.7816	0.7677	1.493
24	Xylenes	21,183	21,595[c]	0.7909	0.7642	1.501
25	Anisole	21,079	21,401[c]	0.8204	0.8173	1.516
26	Tetralin	21,017	21,434[d]	0.8380	0.8083	1.541
27	1-Methylnaphthalene	20,771	21,160[d]	0.9076	0.8829	1.615
Alcohols						
28	Methanol	21,829	22,234[c]	0.6079	0.5904	1.329
29	Ethanol	21,739	22,111[c]	0.6334	0.6239	1.359
30	1-Propanol	21,652	22,026[c]	0.6581	0.6471	1.384
31	2-Propanol	21,739[b]	22,130[c]	0.6334	0.6187	1.377
32	1-Butanol	21,595	21,971[c]	0.6742	0.6620	1.382
33	2- Butanol	21,660[b]	22,028[c]	0.6558	0.6465	1.397
34	*tert*-Butanol	21,745[b]	22,145[c]	0.6317	0.6147	1.386
35	1-Pentanol	21,549	21,936[c]	0.6873	0.6716	1.409
36	2-Pentanol	21,622[b]	21,988[c]	0.6666	0.6574	1.406
37	1-Hexanol	21,511	21,877[c]	0.6980	0.6876	1.418
38	2-Hexanol	21,563[b]	21,942[c]	0.6833	0.6699	1.415
39	1-Octanol	21,459	21,834[c]	0.7127	0.6993	1.429
40	2-Octanol	21,520[b]	21,876[c]	0.6955	0.6879	1.426
41	Cyclopentanol	21,363[b]	21,705[c]	0.7399	0.7345	1.453
42	Benzyl alcohol	20,935	21,262[c]	0.8612	0.8551	1.540
Nitriles						
43	Acetonitrile	21,699	22,080[c]	0.6448	0.6324	1.344
Ethers						
44	Diethyl ether	21,798	22,208[c]	0.6167	0.5975	1.353
45	Di-iso-propyl ether	21,769[b]	22,183[d]	0.6249	0.6043	1.368
46	Di-*n*-butyl ether	21,603[b]	21,922[c]	0.6720	0.6754	1.399
47	1,4-Dioxane	21,372	21,722[c]	0.7374	0.7298	1.422
48	THF	21,455	21,806[c]	0.7139	0.7070	1.407
Ketones						
49	Acetone	21,677	22,007[c]	0.6510	0.6522	1.359
50	2-Butanone	21,613[b]	21,971[c]	0.6691	0.6520	1.379
51	Acetophenone	20,981	21,256[c]	0.8482	0.8568	1.532
Esters						
52	Diethyl carbonate	21,633	21,996[c]	0.6635	0.6552	1.384
53	Propylene carbonate	21,342	21,734[d]	0.7459	0.7266	1.421
54	Ethyl acetate	21,660	22,028[c]	0.6558	0.6465	1.372
Carboxylic acid amides						
55	DMF	21,296	21,604[c]	0.7589	0.7620	1.431
56	DMAc	21,281	21,594[c]	0.7632	0.7647	1.438
Sulfoxides						
57	DMSO	21,047	21,340[c]	0.8295	0.8339	1.479
Pyridines						
58	Pyridine	21,004	21,331[c]	0.8416	0.8363	1.510
Amines						
59	Aniline	20,714	21,039[d]	0.9238	0.9158	1.586

(*continued on next page*)

Table 2 (*continued*)

Entry	Solvent	$\tilde{\nu}_{\mathrm{max,\ ttbP9}}$, cm^{-1}[a]	$\tilde{\nu}_{\mathrm{max,\ \beta\text{-}carotene}}$, cm^{-1}	SP$_{\mathrm{ttbP9}}$	SP$_{\beta\text{-carotene}}$	n[a]
60	Triethylamine	21,644	22,039[c]	0.6603	0.6439	1.400
Miscellaneous solvents						
61	Hexamethylphosphoric acid triamide	21,347[b]	21,592[d]	0.7445	0.7653	1.458
62	Carbon disulfide	20,445	20,730[d]	1.0000	1.0000	1.627
63	Acetic acid	21,676	22,102[c]	0.6513	0.6264	1.369
64	Acetic anhydride	21,529	21,915[c]	0.6929	0.6773	1.390
65	*N*-Methylimidazole	21,031	21,296[c]	0.8340	0.8459	1.529
66	1-Methylpyrrolidin-2-one	21,110	21,415[c]	0.8116	0.8135	1.470
67	Nitromethane	21,470	21,951[c]	0.7096	0.6675	1.379
68	Petroleum ether b.p.: 50–70 °C	21,881	22,267[c]	0.5932	0.5814	1.363
2-Alkoxyethanols						
69	2-Methoxy ethanol	–	21,833[c]	–	0.6996	1.402[e]
70	2-Ethoxy ethanol	–	21,825[c]	–	0.7018	1.408[e]
71	2-Propoxy ethanol	–	21,820[c]	–	0.7032	1.414[e]
72	2-Butoxy ethanol	–	21,806[c]	–	0.7070	1.420[e]
73	2-Pentyloxy ethanol	–	21,800[c]	–	0.7086	1.423[e]
74	2-Hexyloxy ethanol	–	21,781[c]	–	0.7138	1.429[e]
75	2-Octyloxy ethanol	–	21,767[c]	–	0.7176	1.435[e]
76	2-Decyloxy ethanol	–	21,711[c]	–	0.7328	1.450[e]
Ionic liquids						
77	AlHxImCl	–	21,574[c]	–	0.7702	1.5134[c]
78	AlHpImCl	–	21,545[c]	–	0.7781	1.5090[c]
79	AlOcImCl	–	21,527[c]	–	0.7830	1.5061[c]
80	AlDcImCl	–	21,479[c]	–	0.796	1.4889[c]

[a] From Catalán and Hopf (2004) [5].
[b] From Catalán (2009) [6].
[c] Present work.
[d] From Abe et al. (1998) [19].
[e] From Cooper and Partridge (1950) [25].

The same correlations for aliphatic alcohols, 2-alkoxyethnols, and ILs are listed in Eqns. (1)–(6) of item 3 of SM. The relevant point in all these correlations is that the regression coefficients of SP and $f(n^2)$ are similar, a clear indication that β-carotene and $f(n^2)$ respond similarly to solvent polarizability. The advantage of using the probe is that it reports on its *local* solubilization site. Consequently, it can be employed for determining polarizability in cases where $f(n^2)$ is either experimentally inaccessible, or has dubious meaning, e.g., the interfacial region of micellar aggregates; the surfaces of biopolymers, etc.;

(iii) Table 2 contains previously unreported data for 2-alkoxyethanols. In addition to being employed extensively as industrial solvents and in household cleaning formulations [29,30], the bifunctional molecular structure of $ROCH_2CH_2OH$ leads to the formation of several inter- as well as intra-molecular H-bonded species [31]. The strength of these dipolar head-group interactions (on the expense of van der Waals interactions) may explain the larger response of the ROH series to N_C, relative to the 2-alkoxyethanol counterpart;

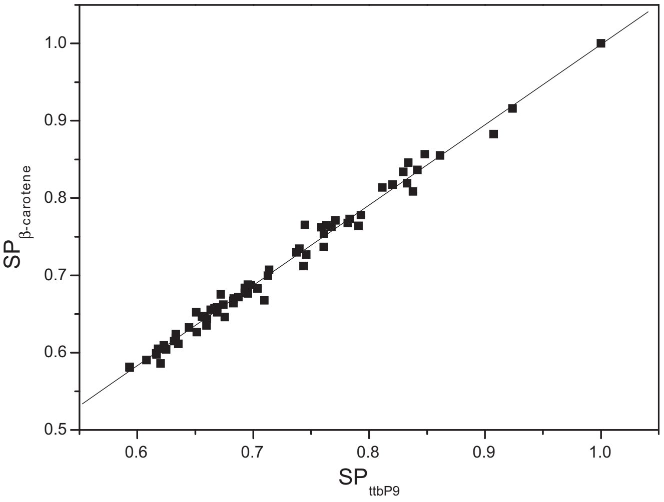

Fig. 7. Correlation between the SP values of ttbP9 and β-carotene.

(iv) Entries 77–80 of Table 2 show (SP) of ILs. Although the number of ILs tested is small, the results show that the dependence of SP on N_C is relatively large, in agreement with the view that dipolar interactions are important for ILs with short side-chain, whereas hydrophobic interactions predominate for ILs with $R > C_6$. That is, ILs and possibly their solutions in some molecular solvents should be regarded as microheterogeneous media, due to the formation of hydrophobic domains, akin to micellar aggregates [32–35].

In summary, the results of theoretical calculations and experimental ones point in the same direction, namely β-carotene and ttbP9 respond similarly to (SP). This similarity, as evidenced by Eqn. (7), and Fig. 7, argues *convincingly, that both probes can be employed interchangeably for the calculation of solvent polarizability.*

4. Conclusions

The green, commercially available, low cost β-carotene can be conveniently employed for the determination of medium polarizability instead of ttbP9 that is obtained by an elaborate, rather expensive synthetic route. Any impurity, if it is present, has no consequence on the spectroscopic parameter of interest, λ_{max} of the solvatochromic peak. The FWHH and shape of the latter are independent of dye concentration, or the nature of solvent. Theoretical calculations of $\tilde{\nu}_{\mathrm{max}}(N_S = 23)$, and experimental correlation between the values of $\tilde{\nu}_{\mathrm{max}}(N_S = 68)$ have shown that both probes are sensitive, *almost to the same extent*, to solvent polarizability. New SP data are reported for important homologous series of molecular solvents and ILs. The dependence of (SP) on N_C of four homologous series shows the importance of solvent head-group interactions (ROEtOH) and that van der Waals interactions are important in ILs. The removal of the synthesis “hurdle” is important for understanding the role of solvent, an important aspect of green chemistry.

5. Calculations

5.1. Geometry optimization of the molecular structures of β-carotene, ttbP9, and the model compounds

The most stable conformations of the natural dye, s-cis form of trans-β-carotene; ttbP9; 2,2,4,4-tetramethylpentane, and 1,2,3,3-tetramethylcyclohexene had their geometries optimized by using DFT calculation that employed B3LYP density functional and 6-31G(d,p) basis set.

For both probes, the transition energies between the fundamental- and excited state were calculated by TD-DFT, using BOP density functional and DH (Dunning/Hay "double zeta") basis set with the application of long-range correction. Values of $\tilde{\nu}_{\text{max}}$ of the excited states with the largest oscillator strength are shown in Table 1. Solvent effects were simulated by using the Polarizable Continuum Model (PCM) combined with SMD solvation model. The solvation free energy, $\Delta G_{\text{solvation}}$, was calculated from the difference between the free energy of the probe (ground state) in the solvent and in the gas phase. All calculations were performed by using the version 1 OCT 2010 (R3) of Gamess program package [36].

5.2. Calculation of solvent SP and reduced $f(n^2)$

The solvent polarizability scale (SP) is calculated by Eqn. (10) [5]:

$$\text{SP} = \frac{\tilde{\nu}_{\text{max gas}} - \tilde{\nu}_{\text{max solvent}}}{\tilde{\nu}_{\text{max gas}} - \tilde{\nu}_{\text{max CS}_2}} \tag{10}$$

where $\tilde{\nu}_{\text{max gas}}$ is the wavenumber of the probe in the gas phase, and $\tilde{\nu}_{\text{max CS}_2}$ is the correspondent value in CS_2. The negligible vapor pressure of both probes precludes a direct determination of $\tilde{\nu}_{\text{max gas}}$. This value was obtained by extrapolating to zero the plot of $\tilde{\nu}_{\text{max}}$ versus $f(n^2)$ for a homologous series of linear alkanes. For β-carotene the resulting equation is:

$$\tilde{\nu}_{\text{max gas}} = 24402 - 9624 f(n^2) \quad (r = 0.99188; \; \text{sd} = 19.3666; \; N_s = 8) \tag{11}$$

The equation for calculating $f(n^2)$ is given in Introduction. The reduced value of this function is given by:

$$\text{Reduced } f(n^2) = \frac{f(n^2)_{\text{solvent}}}{f(n^2)_{\text{CS}_2}} \tag{12}$$

This equation is equivalent to Eqn. (10), because $f(n^2)_{\text{gas}} = 0$.

5.3. Deconvolution of the Uv–vis spectrum of β-carotene

The deconvolution of the absorption bands of β-carotene has been carried out by using five individual vibronic features and assuming they have Gaussian shape, as described elsewhere [37], with the help of Grams/32 v.5 software [26].

Acknowledgments

We thank FAPESP (State of São Paulo Research Foundation) for financial support, and the following for research fellowships: Petrobrás SA (C. Loffredo); CNPq (National Council for Scientific Technological Research) (O. A. El Seoud); CNPq/The Academy of Sciences for the Developing World, TWAS (M. Imran). We thank C. Guizzo for his help.

Appendix A. Supplementary material

Supplementary data related to this article can be found online at http://dx.doi.org/10.1016/j.dyepig.2012.07.017.

References

[1] El Seoud OA. Understanding solvation. Pure Appl Chem 2009;81:697–708.

[2] Reichardt C, Welton T. Solvents and solvent effects in organic chemistry. 4th ed. Weinheim: Wiley: VCH; 2011.

[3] Leo AJ, Hansch C. Role of hydrophobic effects in mechanistic QSAR. Perspect Drug Discov Des 1999;17:1–25.

[4] Martins CT, Lima MS, El Seoud OA. Thermosolvatochromism of merocyanine polarity indicators in pure and aqueous solvents: relevance of solvent lipophilicity. J Org Chem 2006;71:9068–79.

[5] Catalán J, Hopf H. Empirical treatment of the inductive and dispersive components of solute-solvent interactions: the solvent polarizability (SP) scale. Eur J Org Chem 2004:4694–702.

[6] Catalán J. Toward a generalized treatment of the solvent effect based on four empirical scales: dipolarity (SdP, a new scale), polarizability (SP), acidity (SA), and basicity (SB) of the medium. J Phys Chem B 2009;113:5951–60.

[7] Lindman B, Karlström G, Stigsson L. On the mechanism of dissolution of cellulose. J Mol Liquids 2010;156:76–81.

[8] Liu H, Sale KL, Holmes BM, Simmons BA, Singh S. Understanding the interactions of cellulose with ionic liquids: a molecular dynamics study. J Phys Chem B 2010;114:4293–301.

[9] El Seoud OA, Silva VC, Possidonio S, Casarano R, Arêas EPG, Gimenes P. Microwave-assisted derivatization of cellulose, 2 – the surprising effect of the structure of ionic liquids on the dissolution and acylation of the biopolymer. Macromol Chem Phys 2011;212:2541–50.

[10] Gray MR, Tykwinski RR, Stryker JM, Tan X. Supramolecular assembly model for aggregation of petroleum asphaltenes. Energy Fuels 2012;25:3116–24.

[11] Klein D, Kiliçkiran P, Mlynek C, Hopf H, Dix I, Jones PG. A general route to fully terminally *tert*-butylated linear polyenes. Chem Eur J 2010;16:10507–22.

[12] Catalán J, Hopf H, Klein D, Martus M. On the photophysics of polyenes. 1. Bathochromic shifts in their $S_0(1^1A_{g-}) \rightarrow S_2(1^1B_{u+})$ electronic transitions caused by the polarizability of the medium. J Phys Chem A 2008;112:5653–7.

[13] Canuto S, Coutinho K, Trzesniak D. New developments in Monte Carlo/quantum mechanics methodology. The solvatochromism of β-carotene in different solvents. Adv Quantum Chem 2002;41:161–83.

[14] Martins JBL, Durães JA, Sales MJA, Vilela AFA, Silva GM, Gargano R. Theoretical investigation of carotenoid ultraviolet spectra. Int J Quantum Chem 2009;109:739–45.

[15] Ruiz-Anchondo T, Glossman-Mitnik D. Computational characterization of the β-carotene molecule. J Mol Struct THEOCHEM 2012;913:215–20.

[16] Renge I, Sild E. Absorption shifts in carotenoids—influence of index of refraction and submolecular electric fields. J Photochem Photobiol A Chem 2011;218:156–61.

[17] Ouyang S-L, Sun C-L, Zhou M, Li D-F, Wang WW, Qu G-N, et al. Effect of solution concentration on the structured order and optical properties of short-chain polyene biomolecules. Sci China Phys Mech Astron 2010;53:1646–50.

[18] Myers AB, Birge RR. The effect of solvent environment on molecular electronic oscillator strengths. J Chem Phys 1980;73:5314–21.

[19] Abe T, Abboud J-LM, Belio F, Bosch E, Garcia JI, Mayoral JA, et al. Empirical treatment of solvent–solute interactions: medium effects on the electronic absorption spectrum of β-carotene. J Phys Org Chem 1998;11:193–200.

[20] Mancini PM, Pérez AC, Vottero LR. Nonspecific solute–solvent interactions in binary solvent mixtures containing an aprotic hydrogen-bond acceptor and a hydrogen-bond donor: dipolarity/polarizability and refractive index. J Solution Chem 2001;30:695–707.

[21] Mancini PM, Adam CG, Fortunato GG, Vottero LR. A comparison of nonspecific solvent scales. Degree of agreement of microscopic polarity values obtained by different measurement methods. Arkivoc 2007;xvi:266–80.

[22] Armarego WLF, Chai C. Purification of laboratory chemicals. 5th ed. New York: Elsevier; 2003.

[23] Silva PL, Pires PAR, Trassi MAS, El Seoud OA. Solvation in pure liquids: what can be learned from the use of pairs of indicators? J Phys Chem B 2012;112:14976–84.

[24] Lide DR. CRC handbook of chemistry and physics. 85th ed. Boca Raton: CRC Press; 2004.

[25] Cooper FC, Partridge MW. Antituberculous compounds part VI. p-(w-alkoxyalkoxy)-*N*-arylbenxamidines and analogues. J.Chem.Soc 1950:459–64.

[26] Galactic Ind. Corp. Grams/32. Version 5. Salem: 1997.

[27] Laughlin RG, Bunke GM, Eads CD, Laidig WD, Shelley JC. Preparation and physical characterization of pure β-carotene. Chem Phys Lipids 2002;115:63–76.

[28] ACD Labs. Advanced chemistry development (ACD/Labs) software V11.02. Web version of SciFinder scholar. Available from: <http://scifinder.cas.org>; 2012 [accessed 24.03.12].

[29] Traynor MJ, Wilkinson SC, Williams FM. Metabolism of *n*-butoxyethanol in excised human skin in vitro. Toxicol Lett 2008;177:151–5.

[30] Ullmann's encyclopedia of industrial chemistry. Weinheim: Wiley-VCH; 2003.

[31] D'Angelo M, Onori G, Santucci A. Self-association of monohydric alcohols in water: compressibility and infrared absorption measurements. J Chem Phys 1994;100:3107–13.

[32] Urahata SM, Ribeiro MCC. Structure of ionic liquids of 1-alkyl-3-methylimidazolium cations: a systematic computer simulation study. J Chem Phys 2004;120:1855–63.

[33] Urahata SM, Ribeiro MCC. Single particle dynamics in ionic liquids of 1-alkyl-3-methylimidazolium cations. J Chem Phys 2005;122:24511-1–24511-9.

[34] Canongia Lopes JN, Padua AGH. Nanostructural organization in ionic liquids. J Phys Chem B 2006;110:3330–5.

[35] Wang Y, Voth GA. Tail aggregation and domain diffusion in ionic liquids. J Phys Chem B 2006;110:18601–8.

[36] Schmidt MW, Baldridge KK, Boatz JA, Elbert ST, Gordon MS, Jensen JH, et al. General atomic and molecular electronic structure system. J Comput Chem 1993;14:1347–63.

[37] Chen Z, Lee C, Lenzer T, Oum K. Solvent effects on the $S_0(1^1A_{g-}) \rightarrow S_2(1^1B_{u+})$ transition of β-carotene, echinenone, canthaxanthin, and astaxanthin in supercritical CO_2 and CF_3H. J Phys Chem A 2006;110:11291–7.